不同吸积背景下Regular类黑洞的光学外观

报告人：郭 森

黑洞图像研讨会 · 北京

2023 年 12 月 2 日

Outline

1. Introduction
2. Regular BH
3. Optical appearance within sphericial accretion
4. Optical appearance within disk accretion
5. Summary

Introduction

- Two important developments in black hole physics:

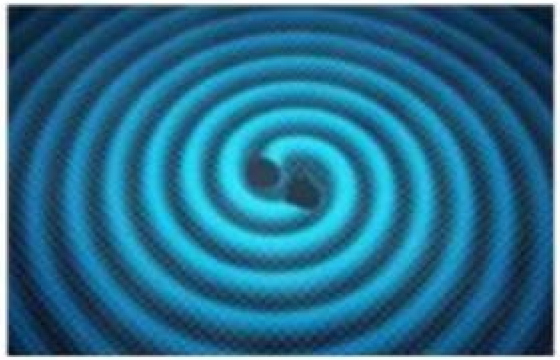

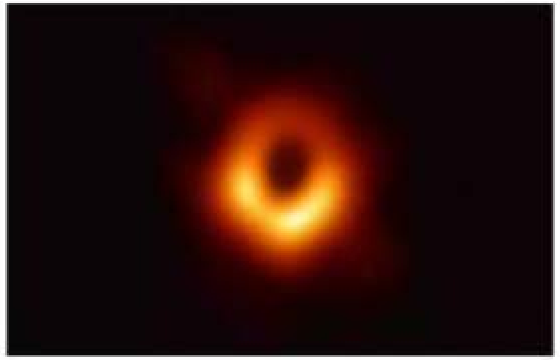

Fig 1: Gravitational wave and shadow of black hole

- LIGO (Laser Interferometer Gravitational-Wave Observatory)

  A collaboration lab between the California Institute of Technology and Massachusetts Institute of Technology

- EHT (Event Horizon Telescope)

  An international collaboration capturing images of black holes using a virtual Earth-sized telescope

Introduction

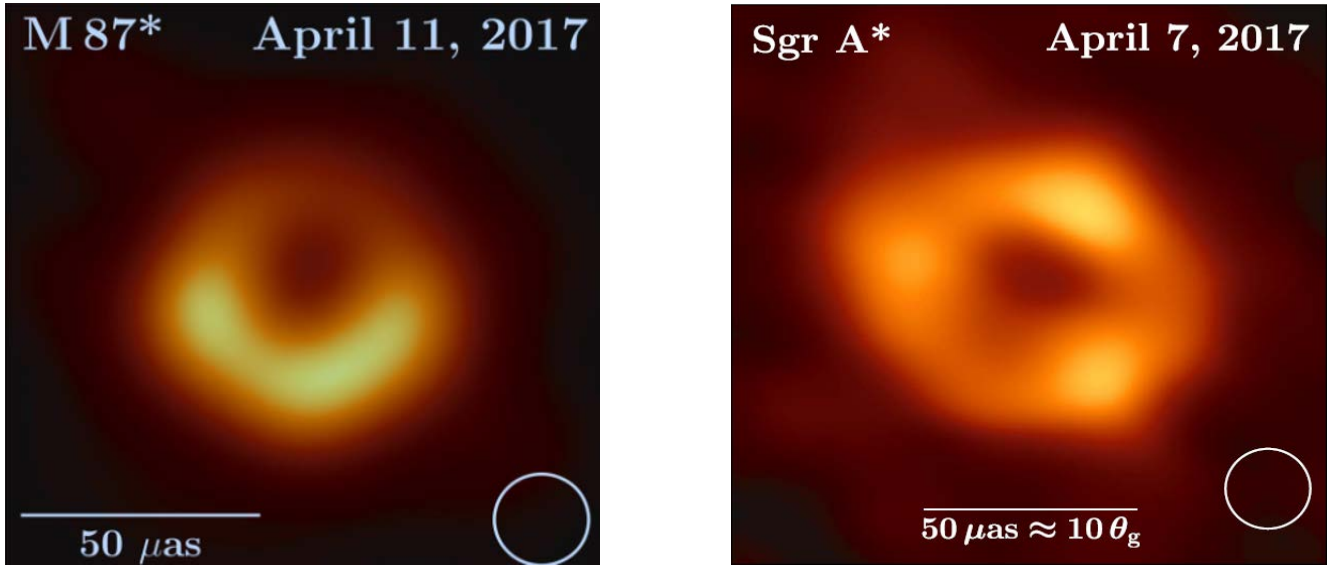

Fig 2: EHT results

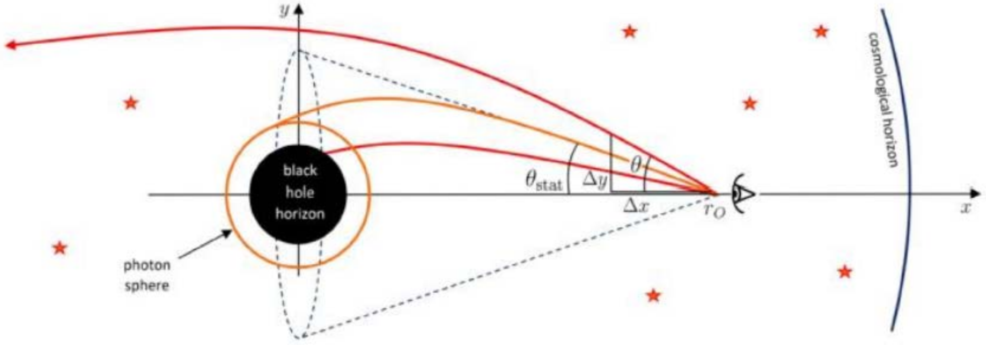

Fig 3: Schematic of light trajectory

- Why is there a shadow in the middle
- Why are there bright rings
- Why the brightness of bright ring is asymmetric

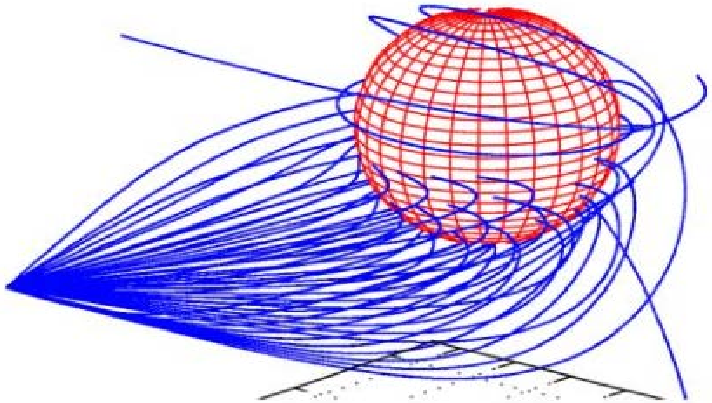

Fig 4: Schematic of ray tracing

Regular BH
- Bardeen introduced a BH solution unaffected by spacetime singularities
- Hayward proposed a regular Hayward BH solution by combining nonlinear electrodynamics with Einstein's field equation

Hayward BH	Bardeen BH
$A_2(r) = 1 - \frac{2Mr^2}{r^3 + g^3},$	$A_3(r) = 1 - \frac{2Mr^2}{(r^2+g^2)^{\frac{3}{2}}},$

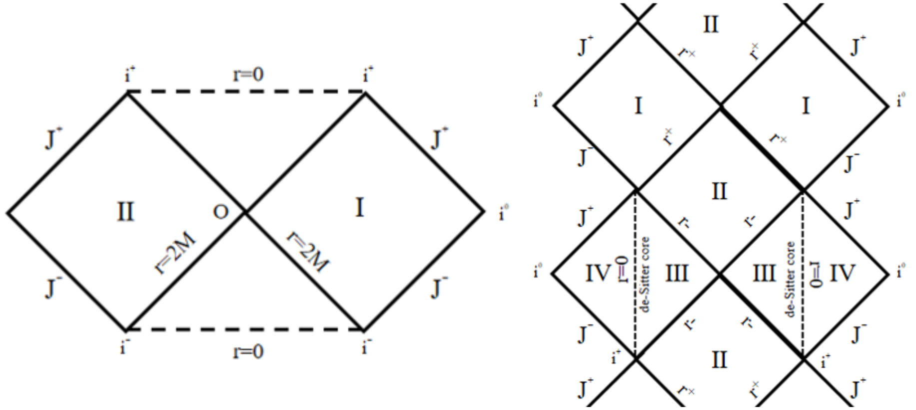

Fig 5: The Carter-Penrose diagram for Schwarzschild BH and regular BH

- With the Euler-Lagrange equation $\frac{d}{d\lambda}\left(\frac{\partial \mathcal{L}}{\partial \dot{x}^\alpha}\right) = \frac{\partial \mathcal{L}}{\partial x^\alpha},$
- Lagrange density $\mathcal{L} = -\frac{1}{2} g_{\alpha\beta} \frac{dx^\alpha}{d\lambda}\frac{dx^\beta}{d\lambda} = \frac{1}{2}\left(f(r)\dot{t}^2 - \frac{\dot{r}^2}{f(r)} - r^2(\dot{\theta}^2 + \sin^2\theta\dot{\psi}^2)\right)$
- Four-component photon $\dot{t} = \frac{1}{bf(r)}, \quad \dot{\phi} = \pm\frac{1}{r^2}, \quad \dot{r}^2 + \frac{f(r)}{r^2} = \frac{1}{b^2}.$
- Radial motion equation $\dot{r}^2 + V(r) = \frac{1}{b^2},$
- Effective potential $V_{\text{eff}} = \frac{1}{r^2}\left(1 - \frac{2Mr^2}{r^3+g^3}\right).$

$$E = -g_{tt}\frac{dt}{d\lambda} = f(r)\frac{dt}{d\lambda},$$

$$L = g_{\psi\psi}\frac{d\psi}{d\lambda} = r^2\frac{d\psi}{d\lambda}.$$

Light deflection of BH

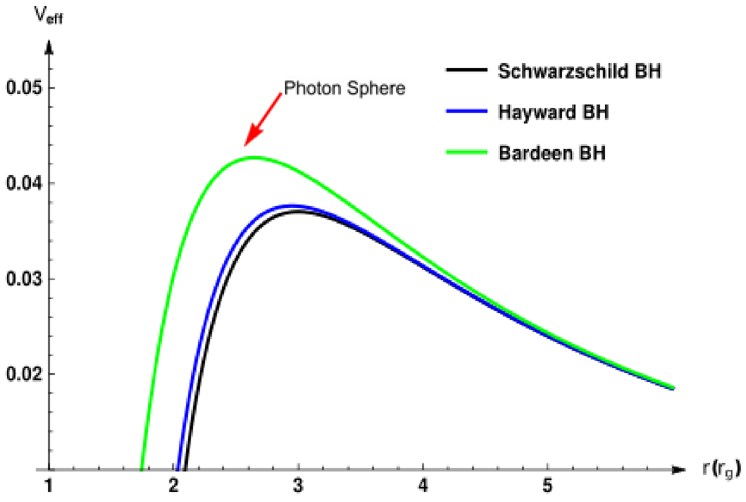

Fig 6: The profile of the effective potential

$$\mathcal{V}_{\rm eff}(r_{\rm ph}) = \frac{1}{b_{\rm ph}^2}, \qquad \mathcal{V}'_{\rm eff}(r_{\rm ph}) = 0,$$

g	0	0.2	0.3	0.5	0.6	0.8
r_+	2	1.99786	1.99321	1.96772	1.94277	1.8504
$r_{\rm ph}$	3	2.99822	2.99397	2.97162	2.95016	2.8747
$b_{\rm ph}$	5.19615	5.19461	5.19094	5.17169	5.15336	5.0901

Tab 1: Hayward BH event horizon r_+ shadow radius r_{ph} and critical impact parameter b_{ph} for different g values in case of a dimensionless BH mass of M=1.

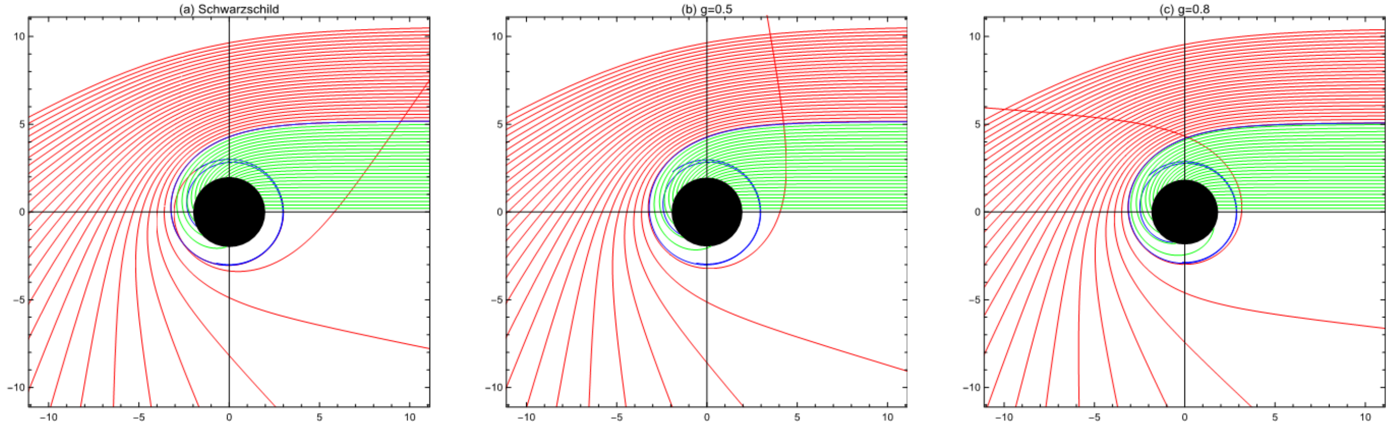

Fig 7: The trajectory of the light ray

Angular size $\delta = (42 \pm 3)\ \mu$as Distance $D = 16.8^{+0.8}_{-0.7}$ Mpc

BH mass $M = (6.5 \pm 0.9) \times 10^9 M_\odot$ Diameter of shadow $d_{M87^*} = \frac{D\delta}{M} \simeq 11.0 \pm 1.5$

Angular size $\delta = (48.7 \pm 7)\ \mu$as Distance $D = (8.15 \pm 0.15)$ kpc

BH mass $M = (4.0^{+1.1}_{-0.6}) \times 10^6 M_\odot$

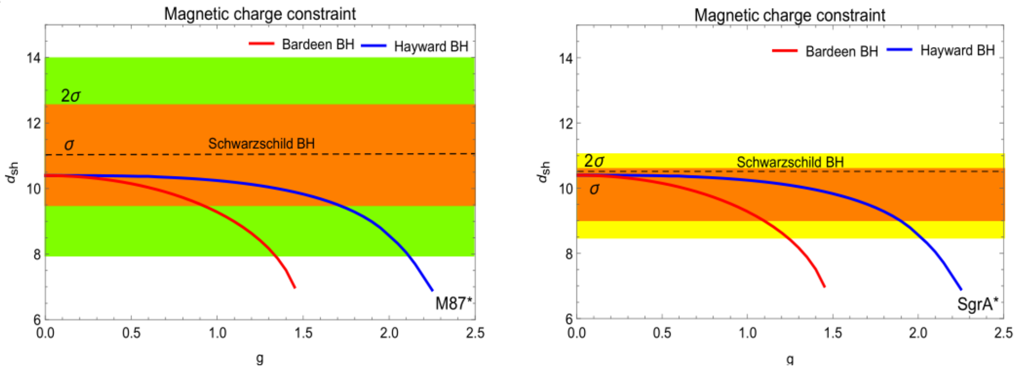

Fig 8: Shadow diameter of the three types BHs as a function of the magnetic charge. The green and orange shaded regions represent the regions of 1σ and 2σ confidence intervals.

Optical appearance within sphericial accretion

The specific intensity observed by the observer (ergs $^{-1}$ cm $^{-2}$ str $^{-1}$ Hz $^{-1}$) can be expressed as

$$I = \int_\gamma g^3 j(\nu_\mathrm{e}) dl_\mathrm{p}$$

in which $g = \nu_\mathrm{o}/\nu_\mathrm{e}$ is the redshift factor, ν_e is the radiated photon frequency and ν_o is the observed photon frequency, $j(\nu_\mathrm{e})$ is the emissivity per unit volume measured in the static frame of the emitter, dl_p is the infinitesimal proper length, and γ stands for the trajectory of the light ray. In the four-dimensional Hayward black hole $g = F(r)^{1/2}$. Concerning the specific emissivity, we also assume that it is monochromatic with rest-frame frequency ν_r, that is

$$j(\nu_\mathrm{e}) \propto \frac{\delta(\nu_e - \nu_r)}{r^2}.$$

The proper length measured in the rest frame of the emitter is $dl_\mathrm{prop} = \sqrt{F(r)^{-1}dr^2 + r^2 d\phi^2} = \sqrt{F(r)^{-1} + r^2 \frac{d\phi}{dr}^2} dr,$

In this case, the specific intensity observed by the infinite observer is

$$\boxed{I(\nu_\mathrm{o}) = \int_\gamma \frac{F(r)^{3/2}}{r^2} \sqrt{F(r)^{-1} + r^2 \frac{d\phi}{dr}^2} dr.}$$

Optical appearance within sphericial accretion

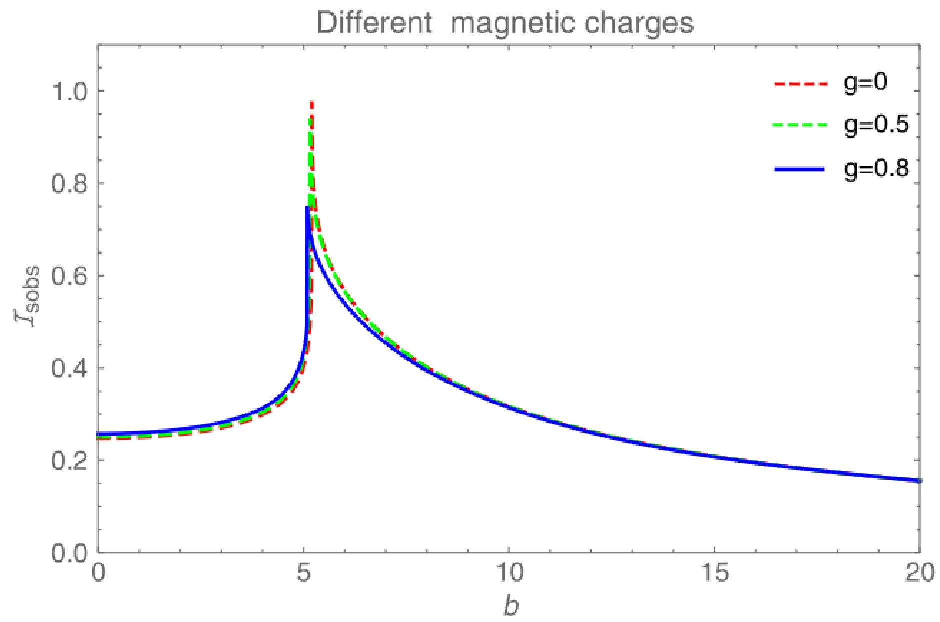

Fig 9: Profiles of the specific intensity I(b) seen by a distant observer for a static spherical accretion

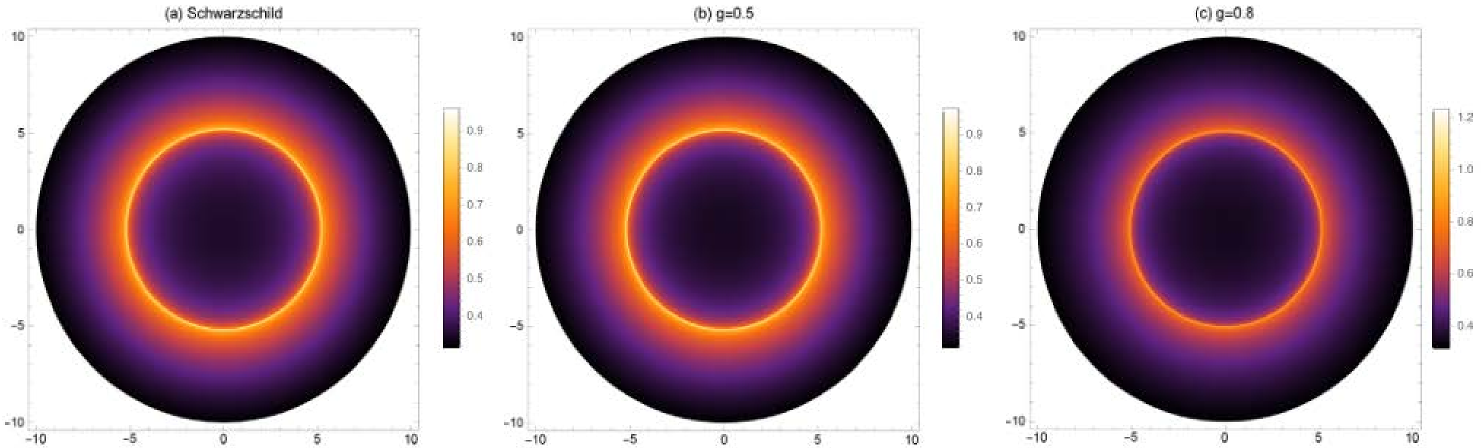

Fig 10: The black hole shadow cast by the static accretion in the (x,y) plane. The bright ring is the photon sphere.

Optical appearance within sphericial accretion

We will also employ the following equation to investigate the intensity

$$I = \int_{\gamma} g^3 j(\nu_{\mathrm{e}}) dl_{\mathrm{p}}$$

Different from the static accretion, the redshift factor for the infalling accretion should be evaluated from

$$g = \frac{k_\beta u_{\mathrm{o}}^\beta}{k_\gamma u_{\mathrm{e}}^\gamma},$$

in which $k^\mu = \dot{x}_\mu$ is the four-velocity of the photon, $u_{\mathrm{o}}^\mu = (1,0,0,0)$ is the 4-velocity of the distant observer, while u_{e}^μ is the 4-velocity of the accretion under consideration

$$u_{\mathrm{e}}^t = \frac{1}{F(r)}, u_{\mathrm{e}}^r = -\sqrt{1-F(r)}, u_{\mathrm{e}}^\theta = u_{\mathrm{e}}^\phi = 0.$$

The four-velocity of the photon has been obtained previously

$$\frac{k_r}{k_t} = \pm\frac{1}{F(r)}\sqrt{1-\frac{b^2 F(r)}{r^2}},$$

Optical appearance within sphericial accretion

With this equation, the redshift factor in above equation can be simplified as

$$g = \frac{1}{u_e^t + k_r/k_e u_e^r}.$$

In addition, the proper distance can be defined by

$$dl_{\text{prop}} = k_\gamma u_e^\gamma d\lambda = \frac{k_t}{g|k_r|}dr,$$

The intensity thus can be expressed as

$$\boxed{I(\nu_o) \propto \int_\gamma \frac{g^3 k_t dr}{r^2|k_r|}.}$$

g	0	0.2	0.5	0.6	0.8
Static	0.97647	0.95314	0.88733	0.77108	0.75055
Infalling	0.00198	0.00201	0.00226	0.00239	0.00241

Tab 2: The total photon intensity of the Hayward BH with static and infalling spherical accretion flows under different values of g for M = 1.

Optical appearance within sphericial accretion

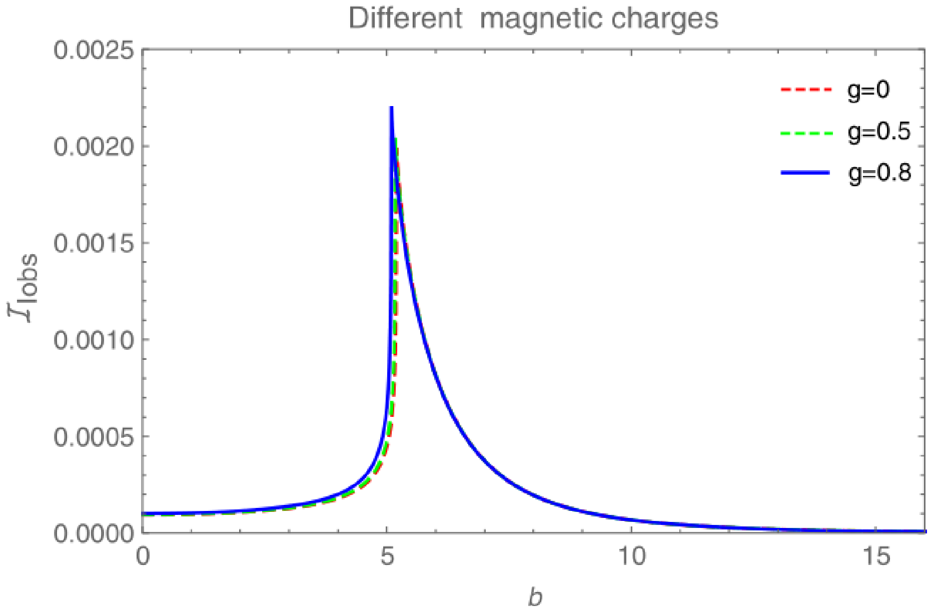

Fig 11: Profiles of the specific intensity I(b) seen by a distant observer for a infalling spherical accretion

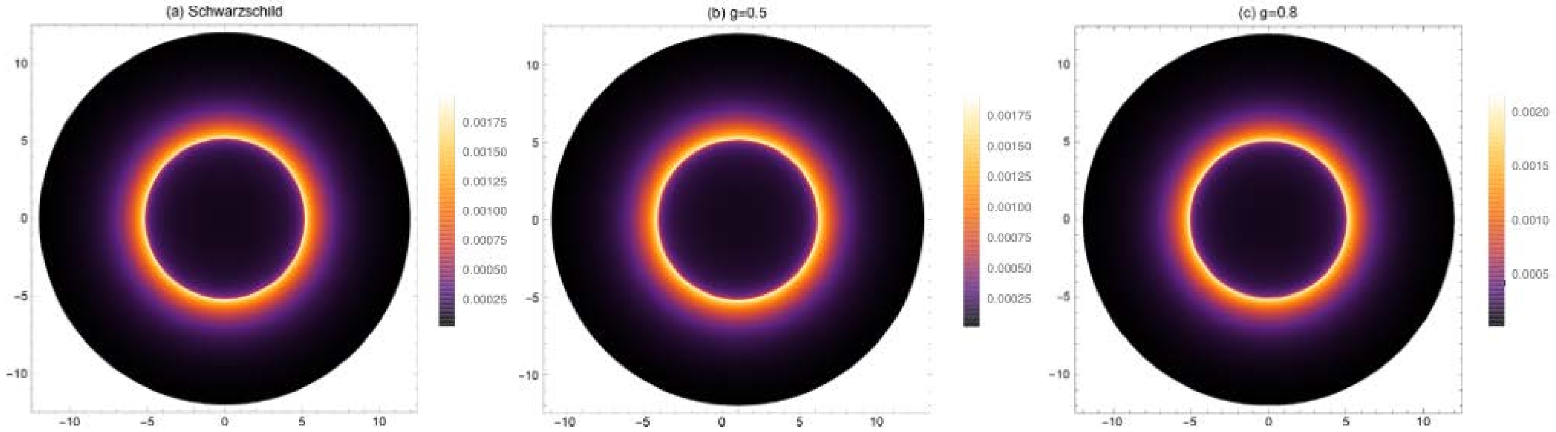

Fig 12: The black hole shadow cast by the infalling accretion in the (x,y) plane. The bright ring is the photon sphere.

Optical appearance within disk accretion

- Optically thin and geometrically thin

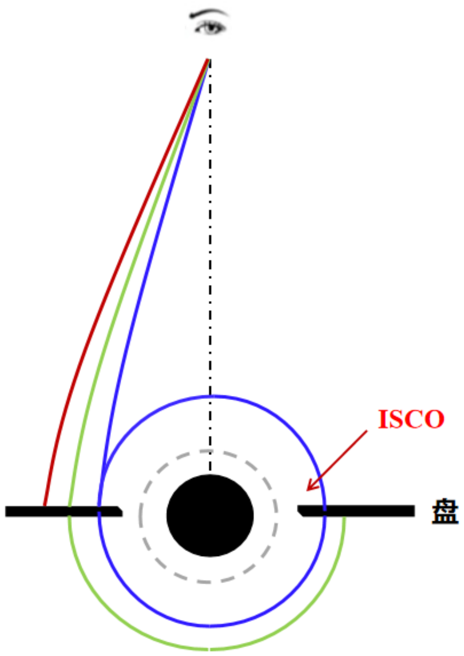

Fig 13: Thin disk model

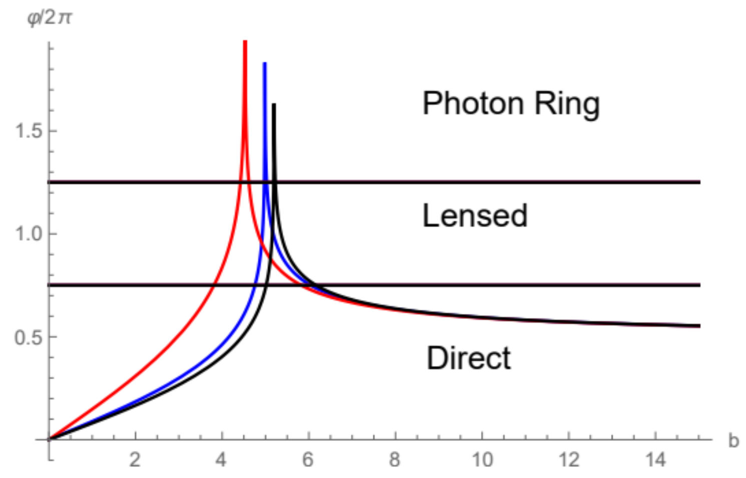

Fig 14: Orbit number as a function of the impact parameter for the BH

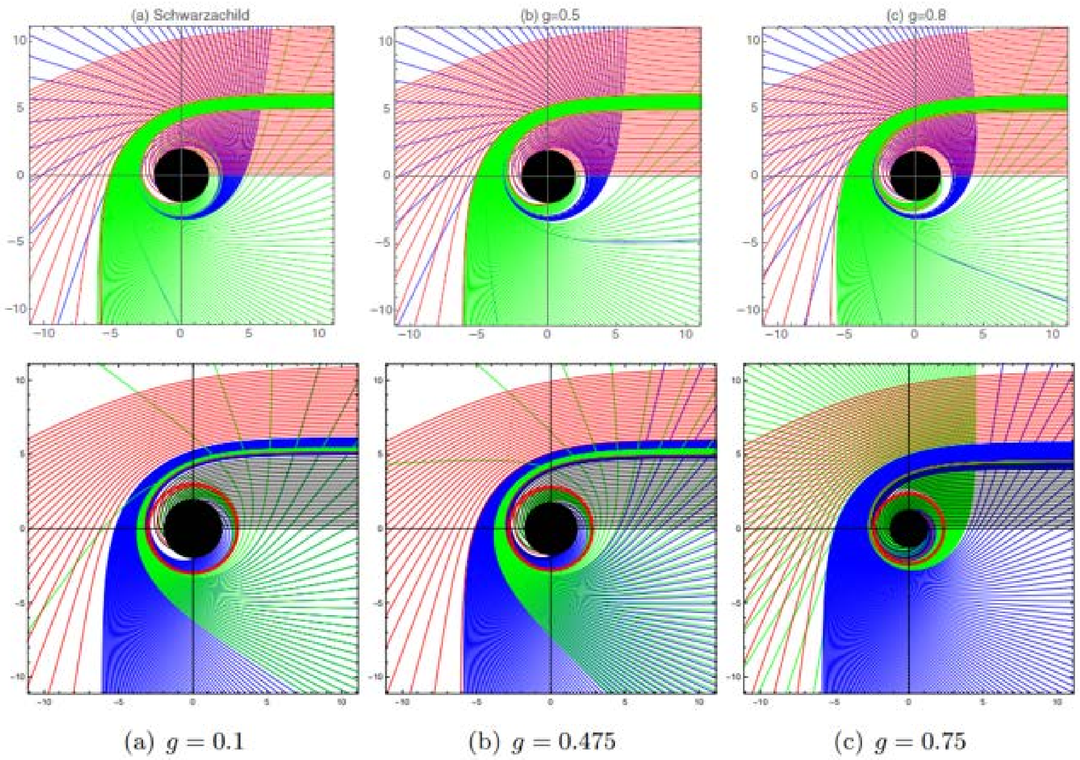

Fig 15: The selection of associated photon trajectories for Hayward BH in the polar coordinates (b,ψ)

Optical appearance within disk accretion

For a single frequency, the observed photon specific intensity can be written as

$$I_{\text{obs}}^{\text{d}}(r) = f(r)^{3/2} I_{\text{em}}^{\text{d}}(r) = \left(1 - \frac{2Mr^2}{r^3 + g^3}\right)^{3/2} I_{\text{em}}^{\text{d}}(r).$$

The total photon intensity can be obtained by integrating over the whole range of received frequencies

$$\begin{aligned} I_{\text{O}} &= \int I_{\text{obs}}^{\text{d}}(r) \mathrm{d}v_{\text{obs}}^{\text{d}} = \int f(r)^2 I_{\text{em}}^{\text{d}}(r) \mathrm{d}v_{\text{em}}^{\text{d}} \\ &= \left(1 - \frac{2Mr^2}{r^3 + g^3}\right)^2 I_{\text{emi}}^{\text{d}}(r), \end{aligned} \longrightarrow \quad I_{\text{emi}}^{\text{d}}(r) \equiv \int I_{\text{em}}^{\text{d}}(r) \mathrm{d}v_{\text{em}}^{\text{d}}$$

The total observed intensity can be written as

$$\boxed{I_{\text{O}} = \sum_n \left(1 - \frac{2Mr^2}{r^3 + g^3}\right)^2 I_{\text{emi}}^{\text{d}}(r)\Big|_{r=r_{\text{n}}(b)},}$$

$$I_{\rm O} = \sum_n \left(1 - \frac{2Mr^2}{r^3 + g^3}\right)^2 I^{\rm d}_{\rm emi}(r)|_{r=r_{\rm n}(b)},$$

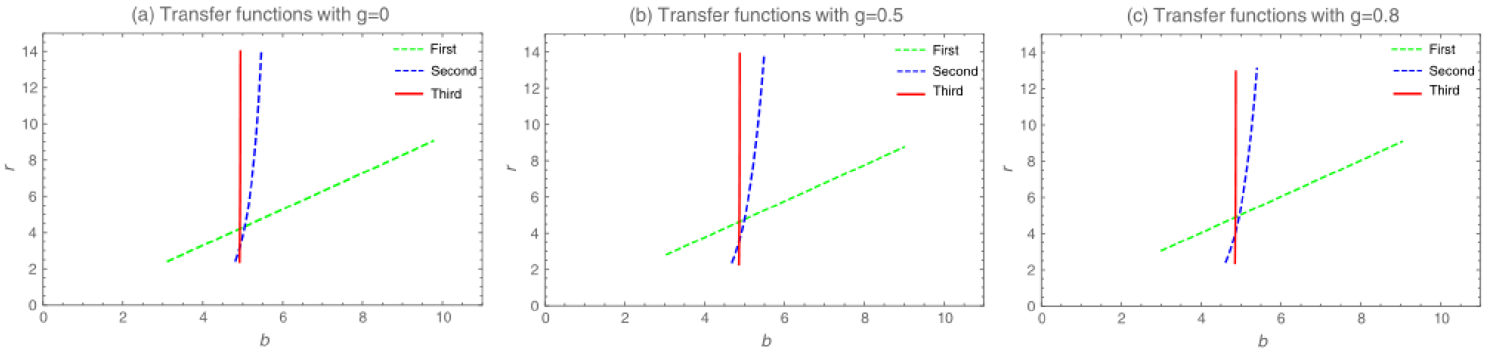

Fig 16: Transfer functions of the Hayward BH

$$I'_{emi}(r) = \begin{cases} \left(\frac{1}{r-(r_{isco}-1)}\right)^2, & r > r_{isco} \\ 0, & r \leq r_{isco} \end{cases}$$

$$I''_{emi}(r) = \begin{cases} \left(\frac{1}{r-(r_p-1)}\right)^3, & r > r_p \\ 0, & r \leq r_p \end{cases}$$

$$I'''_{emi}(r) = \begin{cases} \frac{\frac{\pi}{2}-\tan^{-1}(r-(r_{isco}-1))}{\frac{\pi}{2}+\tan^{-1}(r_p)}, & r > r_+ \\ 0, & r \leq r_+ \end{cases}$$

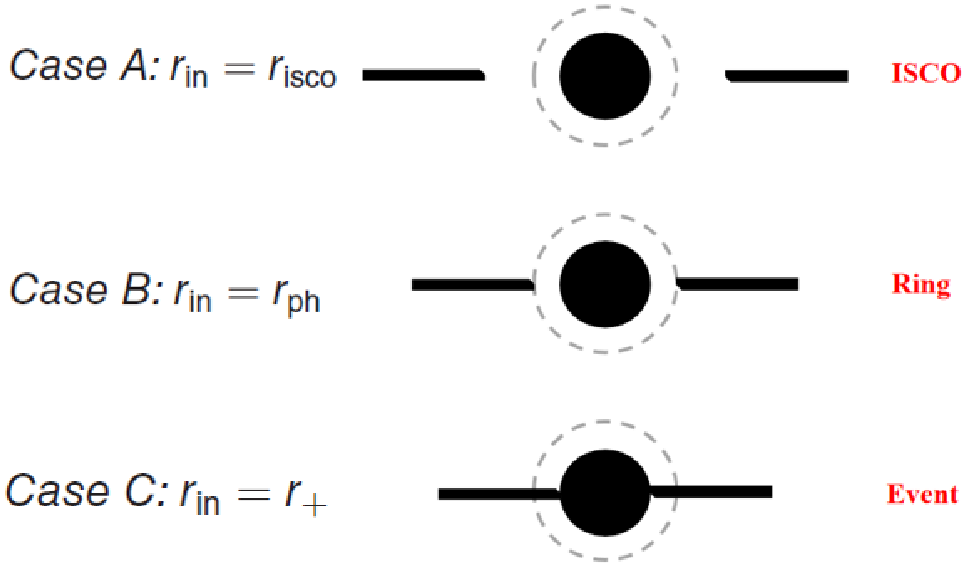

$$I_{\rm emit}(r) = \begin{cases} e^{\frac{-(r-r_{\rm in})^2}{8}} & r > r_{\rm in}, \\ 0 & r \leqslant r_{\rm in}, \end{cases}$$

Optical appearance within thin disk accretion

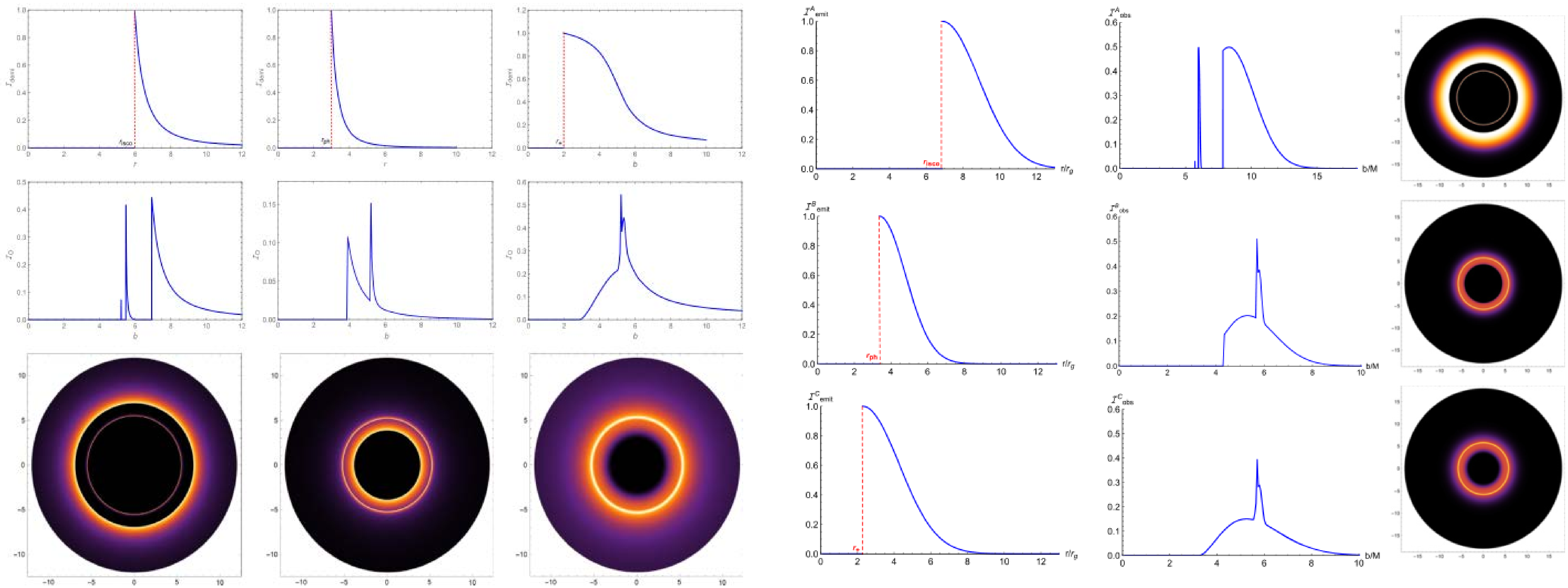

Fig 17: The images of the shadows and the rings for the Hayward BH with a thin disk accretion

Optical appearance within disk accretion

g/I_{demi}	$I'_{\mathrm{demi}}(r)$			$I''_{\mathrm{demi}}(r)$			$I'''_{\mathrm{demi}}(r)$		
Emission	Direct	Lensed	Photon	Direct	Lensed	Photon	Direct	Lensed	Photon
0	0.967	0.0493	0.00926	0.906	0.0184	0.00197	0.956	0.0552	0.00566
0.2	0.954	0.0465	0.00745	0.907	0.0179	0.00182	0.949	0.0542	0.00556
0.5	0.948	0.0428	0.00563	0.909	0.0141	0.00154	0.943	0.0538	0.00552
0.6	0.942	0.0387	0.00455	0.907	0.0123	0.00136	0.936	0.0535	0.00549
0.8	0.936	0.0344	0.00242	0.908	0.0111	0.00115	0.923	0.0531	0.00546

Tab 3: The total observed intensity corresponding to direct emission, lensed ring and photon ring of the Hayward BH with thin disk accretion, where the BH mass as M = 1 and the magnetic charge taking as g = 0, 0.2, 0.5, 0.6, 0.8.

- Ref: Black Hole Shadows, Photon Rings, and Lensing Rings, S. E. Gralla et.al, ***Phys. Rev. D.*** 100 024018 (2019)
- Our works:

1. Influence of accretion flow and magnetic charge on the observed shadows and rings of the Hayward black hole,
S. Guo, G. R. Li, and E. W, Liang, ***Phys. Rev. D.*** 105. 023024 (2022)
2. Observable characteristics of the charged black hole surrounded by thin disk accretion in Rastall gravity
S. Guo, E-W Liang, et.al, ***Class. Quant. Grav.*** 39. 135004 (2022)
3. The shadow and photon sphere of the charged black hole in Rastall gravity
S. Guo, et.al, ***Class. Quant. Grav.*** 38. 165013 (2021)
4. QED and accretion flow models effect on optical appearance of Euler–Heisenberg black holes
X. X. Zeng, **S. Guo***, et.al, ***Eur. Phys. Jour. C.*** 82. 764 (2022)

- Optically thick and geometrically thin

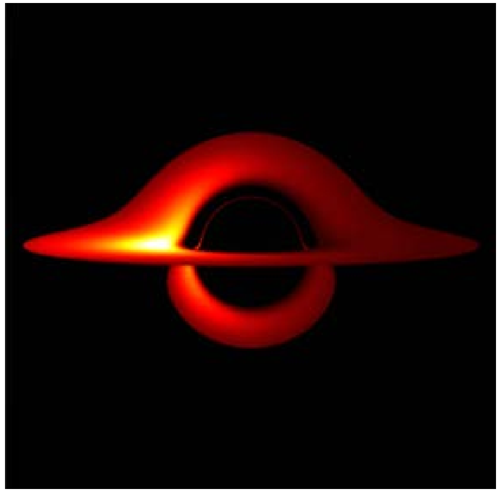

Fig 18: Numerical simulation image of the Schwarzschild BH with a thickness disk accretion

$$\Omega(u) \equiv \frac{\mathrm{d}u}{\mathrm{d}\psi} = \sqrt{\frac{1}{b^2} - u^2\left[1 - \frac{2M}{u^2(g^3 + \frac{1}{u^3})}\right]}.$$

Cardano formula

$$\left(\frac{du}{d\psi}\right)^2 = \frac{2M}{g^3 + \frac{1}{u^3}} - u^2 + \frac{1}{b^2} \equiv 2MG(u) = 2M(u-u_1)(u-u_2)(u-u_3)$$

- *Case 1* $b > b_c : u_1 \leq 0 < u_2 < u_3.$
- *Case 2* $b = b_c : u_1 = -\frac{1}{6M}, u_2 = u_3 = \frac{1}{3M}$
- *Case 3* $b < b_c : u_1 \leq 0, u_2$ *and* u_3 *complex conjugate*

$$u_1 = \frac{P - 2M - Q}{4MP}, \quad u_2 = \frac{1}{P}, \quad u_3 = \frac{P - 2M + Q}{4MP},$$

The bending angle of the light ray is

$$\psi(u) = \sqrt{\frac{2}{M}} \int_0^{u_2} \frac{\mathrm{d}u}{\sqrt{(u-u_1)(u-u_2)(u-u_3)}} - \pi.$$

Semi-analytical methods

$$\psi(u) = \sqrt{\frac{2}{M}}\left(\frac{2F(\Psi_1,k)}{\sqrt{u_3-u_1}} - \frac{2F(\Psi_2,k)}{\sqrt{u_3-u_1}}\right) - \pi,$$

Numerical integration methods

$$\psi = \int_{u_{\rm source}}^{u_{\rm obs}} \Omega(u) = \int_{u_{\rm source}}^{u_{\rm obs}} \frac{\mathrm{d}u}{\sqrt{\frac{1}{b^2} - u^2 A(u)}}$$

Optical appearance within disk accretion

For the (1 + n)*th* order image of the accretion disk is

$$2n\pi - \gamma = 2\sqrt{\frac{P}{Q}}\Big(2K(k) - F(\zeta_{\mathrm{r}}, k) - F(\zeta_{\infty}, k)\Big),$$

in which *K(k)* is the complete elliptic integral

- Numerical integration algorithms

$$\cos\phi = -\frac{\sin\eta\tan\theta_0}{\sqrt{\sin^2\eta\tan^2\theta_0 + 1}},$$

$$\sin\phi = -\frac{1}{\sqrt{\sin^2\eta\tan^2\theta_0 + 1}},$$

For the (1 + n)*th* order image of the accretion disk is

$$\int_{u_{\mathrm{source}}}^{u_{\mathrm{obs}}} \frac{\mathrm{d}u}{\sqrt{\frac{1}{b^2} - u^2 A(u)}} = k\pi - \arccos\frac{\sin\eta\tan\theta_0}{\sqrt{\sin^2\eta\tan^2\theta_0 + 1}},$$

Optical appearance within disk accretion

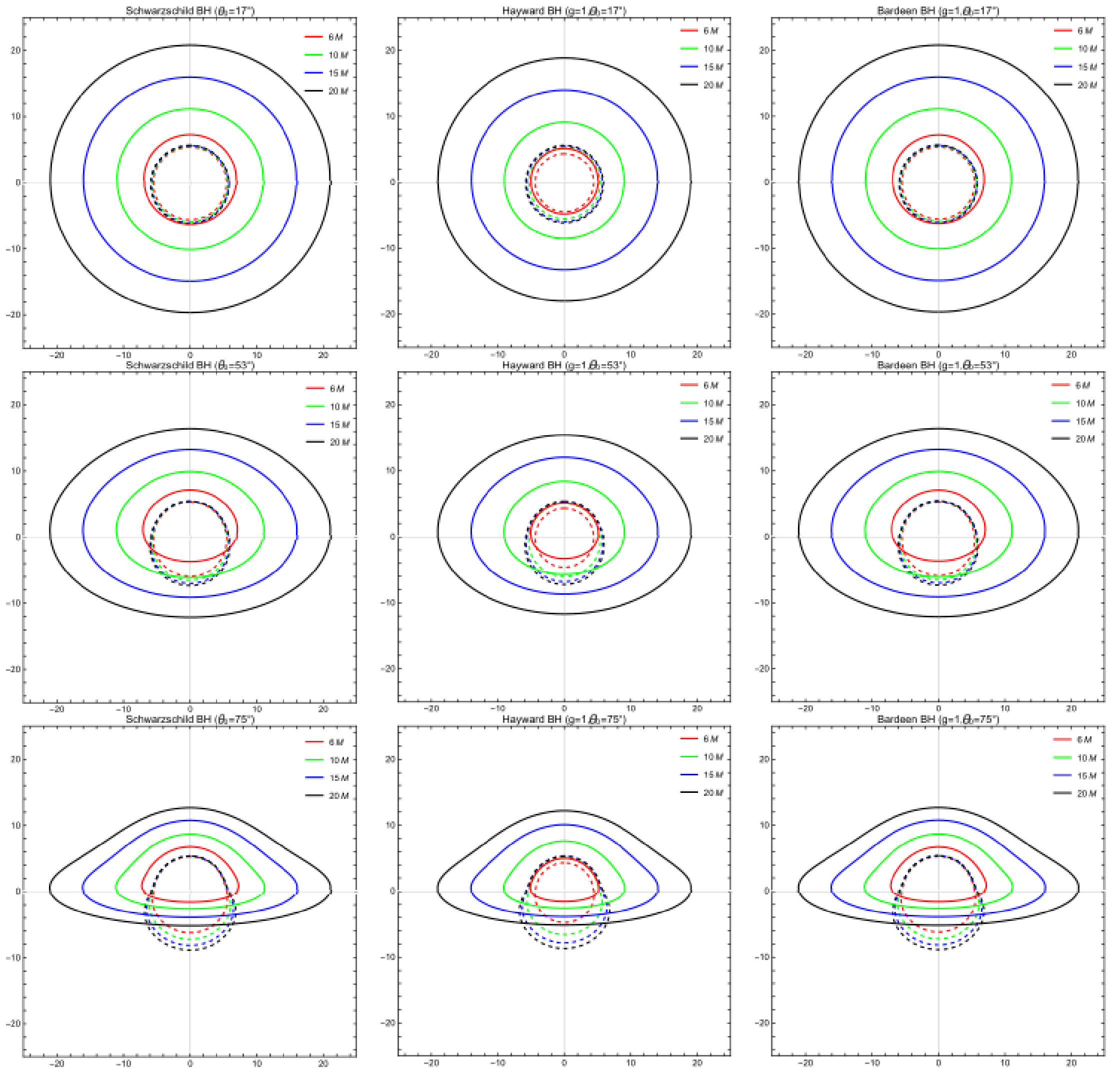

Fig 19: The direct (solid line) and secondary (dashed line) images of BHs accretion disks with different the observation angles. The BH mass is taken as $M = 3M_\odot$ and magnetic charge is $g = 1$

Optical appearance within disk accretion

The radial dependence of energy flux radiated by a thin accretion disk around a BH is

$$F = -\frac{\dot{M}}{4\pi\sqrt{-\mathrm{g}}}\frac{\Omega_{,\mathrm{r}}}{(E-\Omega L)^2}\int_{r_{\mathrm{in}}}^{r}(E-\Omega L)L_{,\mathrm{r}}\mathrm{d}r,$$

$$E = -\frac{g_{tt}+g_{t\phi}\Omega}{\sqrt{-g_{tt}+2g_{t\phi}\Omega-g_{\phi\phi}\Omega^2}},$$

$$L = \frac{g_{t\phi}+g_{\phi\phi}\Omega}{\sqrt{-g_{tt}+2g_{t\phi}\Omega-g_{\phi\phi}\Omega^2}},$$

$$\Omega = \frac{\mathrm{d}\phi}{\mathrm{d}t} = \frac{-g'_{t\phi}+\sqrt{(g'_{t\phi})^2-g'_{tt}g'_{\phi\phi}}}{g'_{\phi\phi}}.$$

The observed flux F_{obs} is different from the source F duo to the redshift

$$F_{\mathrm{obs}} = \frac{F}{(1+z)^4}.$$

The redshift factor is

$$d = 1+z = \frac{E_{\mathrm{em}}}{E_{\mathrm{obs}}} = \frac{1+b\Omega\cos\beta}{\sqrt{-g_{tt}-2g_{t\phi}-g_{\phi\phi}}}.$$

Optical appearance within disk accretion

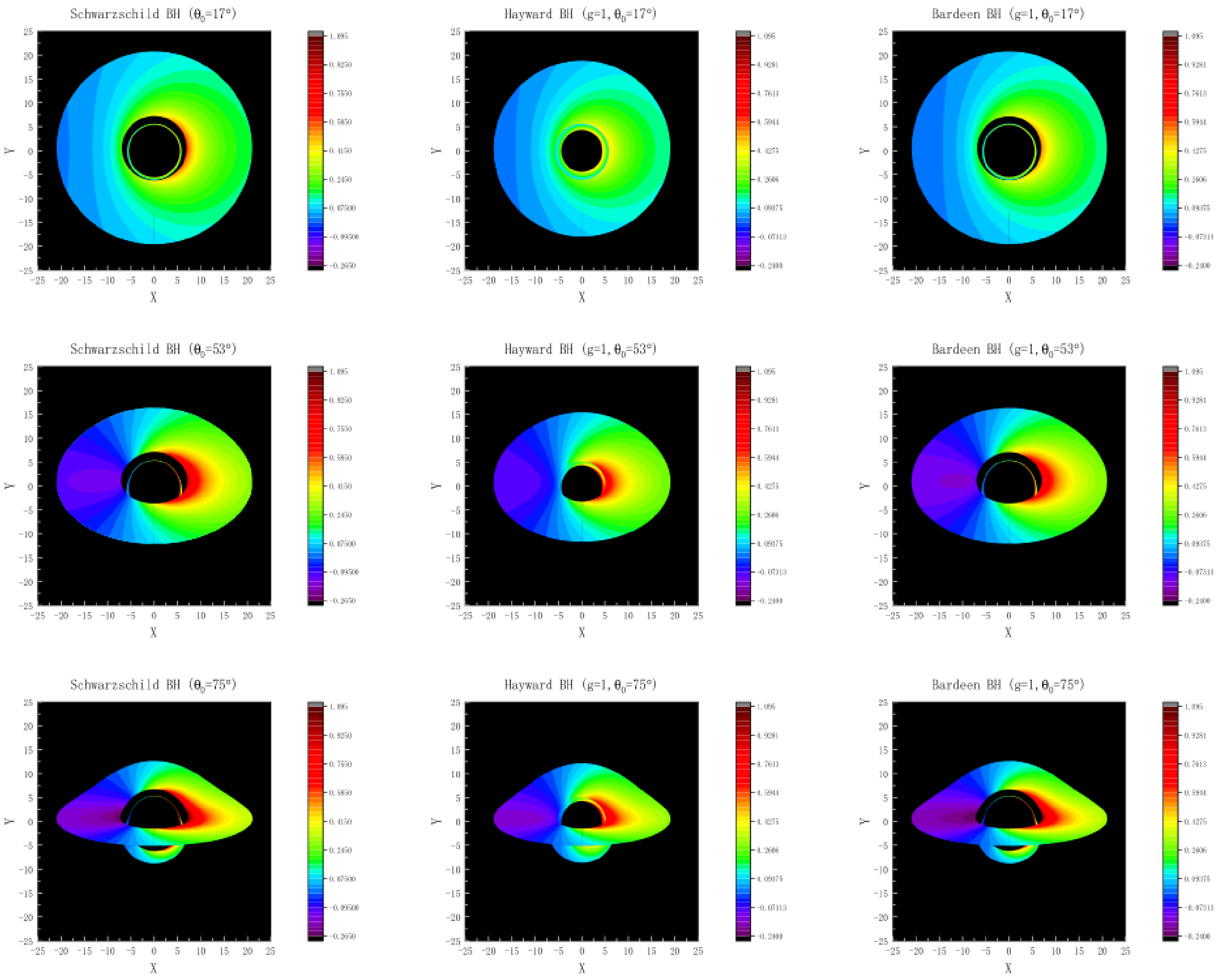

Fig 20: Redshift distribution (curves of constant redshift z) of the accretion disk around Schwarzschild and Regular BHs

Optical appearance within disk accretion

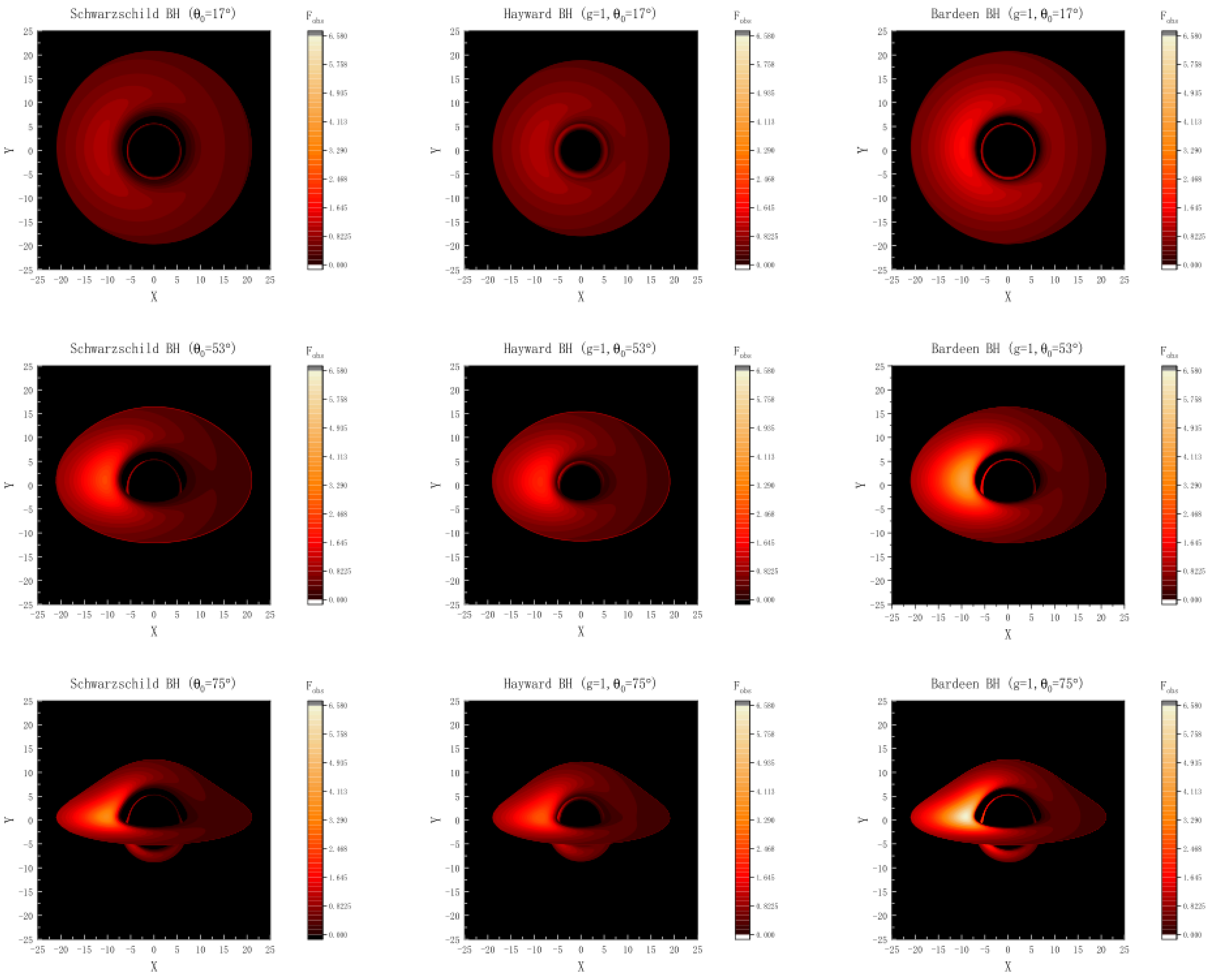

Fig 21: Direct and secondary images of the accretion disk around Schwarzschild and Regular BH

- Our works:

1. Unveiling the unconventional optical signatures of regular black holes within accretion disk
S. Guo, E. W, Liang, et.al,
Eur. Phys. Jour. C. 83. 1059 (2023)

2. Influence of accretion disk on the optical appearance of the Kazakov-Solodukhin black hole
Y. X. Huang, **S. Guo***, et.al,
Phys. Rev. D. 107. 123009 (2023)

Optical appearance within disk accretion

Fourier function:

$$F_1(x) = a_1 + b_1\cos(hx) + c_1\sin(hx) + d_1\cos(2hx) \\ +e_1\sin(2hx) + f_1\cos(3hx) + g_1\sin(3hx),$$

Gaussian function:

$$F_2 = a_2 e^{-\left(\frac{x-b_2}{c_2}\right)^2} + d_2 e^{-\left(\frac{x-e_2}{f_2}\right)^2} + g_2 e^{-\left(\frac{x-h_2}{i_2}\right)^2},$$

Exponential function:

$$F_3 = a_3 e^{b_3 x} + c_3 e^{d_3 x},$$

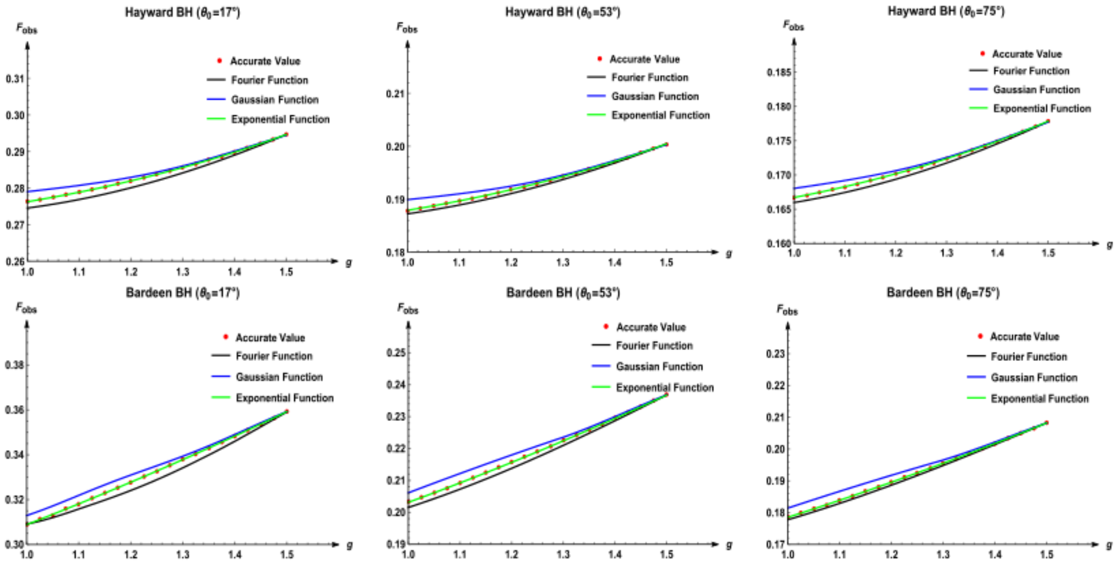

−	a_3	b_3	c_3	d_3
F	2.0391	−7.0162	0.4113	0.2977
$F_{obs}(\theta_0 = 17°)$	0.0207	−1.0981	0.2182	0.3253
$F_{obs}(\theta_0 = 53°)$	0.1193	−4.6926	0.1473	0.3161
$F_{obs}(\theta_0 = 75°)$	0.3207	−5.9462	0.1295	0.3165

−	a_3	b_3	c_3	d_3
F	0.4074	−0.1822	0.0725	0.7019
$F_{obs}(\theta_0 = 17°)$	0.2317	−0.1793	0.0408	0.7062
$F_{obs}(\theta_0 = 53°)$	0.1578	−0.1784	0.0275	0.7095
$F_{obs}(\theta_0 = 75°)$	0.1412	−0.1787	0.0244	0.7096

Tab 4: Regular BH coefficient value of exponential fitting

$$A_1 \sim -2.2; \quad B_1 \sim 2.5; \quad C_1 \sim -0.19; \quad D_1 \sim -0.01$$

$$A_2 \sim 0.23; \quad B_2 \sim 2.38; \quad C_2 \sim 0.004$$

$$D_2 \sim -0.008; \quad E_2 \sim 0.43; \quad F_2 \sim 1.39$$

$$A_3 \sim -3 * 10^{-4}; \quad B_3 \sim 8 * 10^{-4}; \quad C_3 \sim -2 * 10^{3}$$

$$D_3 \sim -3 * 10^{-3}; \quad E_3 \sim -2 * 10^{-2}; \quad F_3 \sim 8 * 10^{-6}; \quad G_3 \sim 0.2$$

Optical appearance within thin disk accretion

- Thin-shell wormhole with a Regular profile

The two spherically symmetric metrics are connected by the throat

$$f_i(r_i) = 1 - \frac{2M_i r_i^2}{r_i^3 + g_i^3}, \quad r \geq R,$$

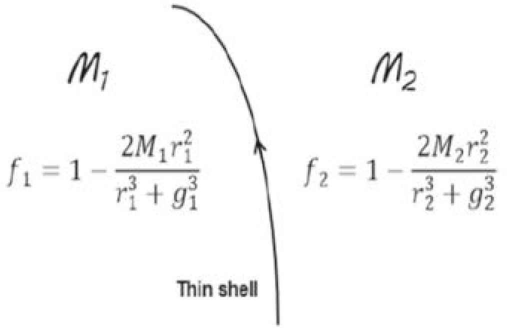

Fig 23: A TSW with a Hayward profile serves as a mimic of a BH

The effective potential V_{eff} of a TSW with a Hayward profile

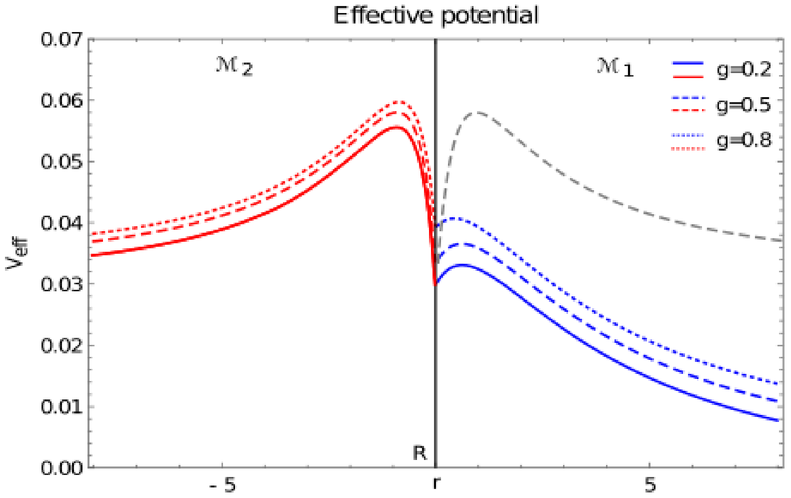

Fig 22: Effective potential of a TSW with a Hayward profile as a function of radius

The total change of azimuthal angle

$$\phi_1(b_1) = 2\int_0^{u_1^{\min}} \frac{du_1}{\sqrt{\Omega_1(u_1)}}, \quad b_1 > b_{c_1}.$$

$$\phi_1^*(b_1) = \int_0^{1/R} \frac{du_1}{\sqrt{\Omega_1(u_1)}}, \quad b_1 < b_{c_1}.$$

$$\phi_2(b_2) = 2\int_{u_2^{\max}}^{1/R} \frac{du_2}{\sqrt{\Omega_2(u_2)}}, \quad b_2 > b_{c_2}.$$

- Our works:

1. Optical appearance of a thin-shell wormhole with a Hayward profile
S. Guo, E. W. Liang, et.al,
Eur. Phys. Jour. C. 83. 663 (2023)

Optical appearance within disk accretion

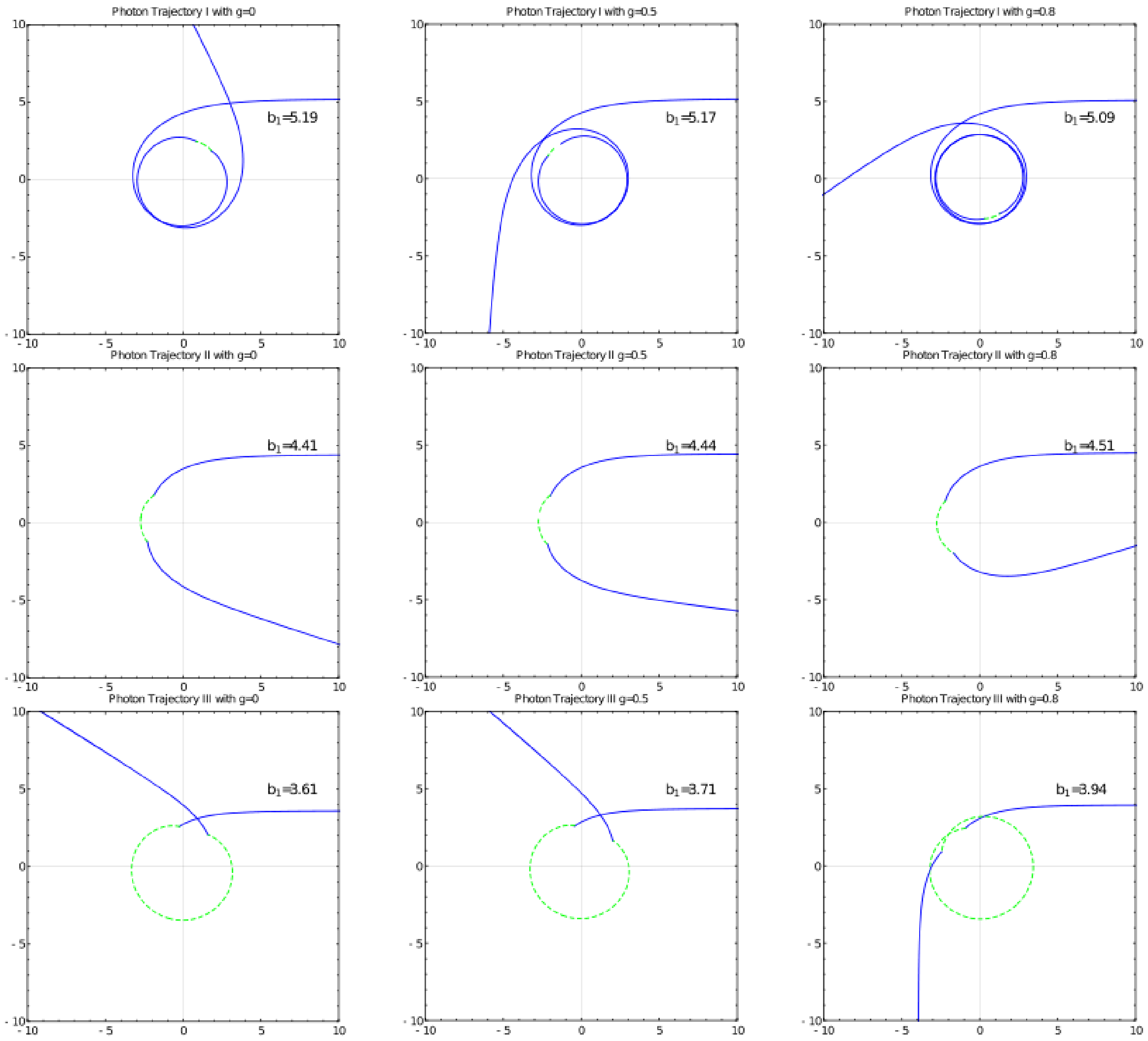

Fig 24: Light trajectories of TSW with a Hayward profile

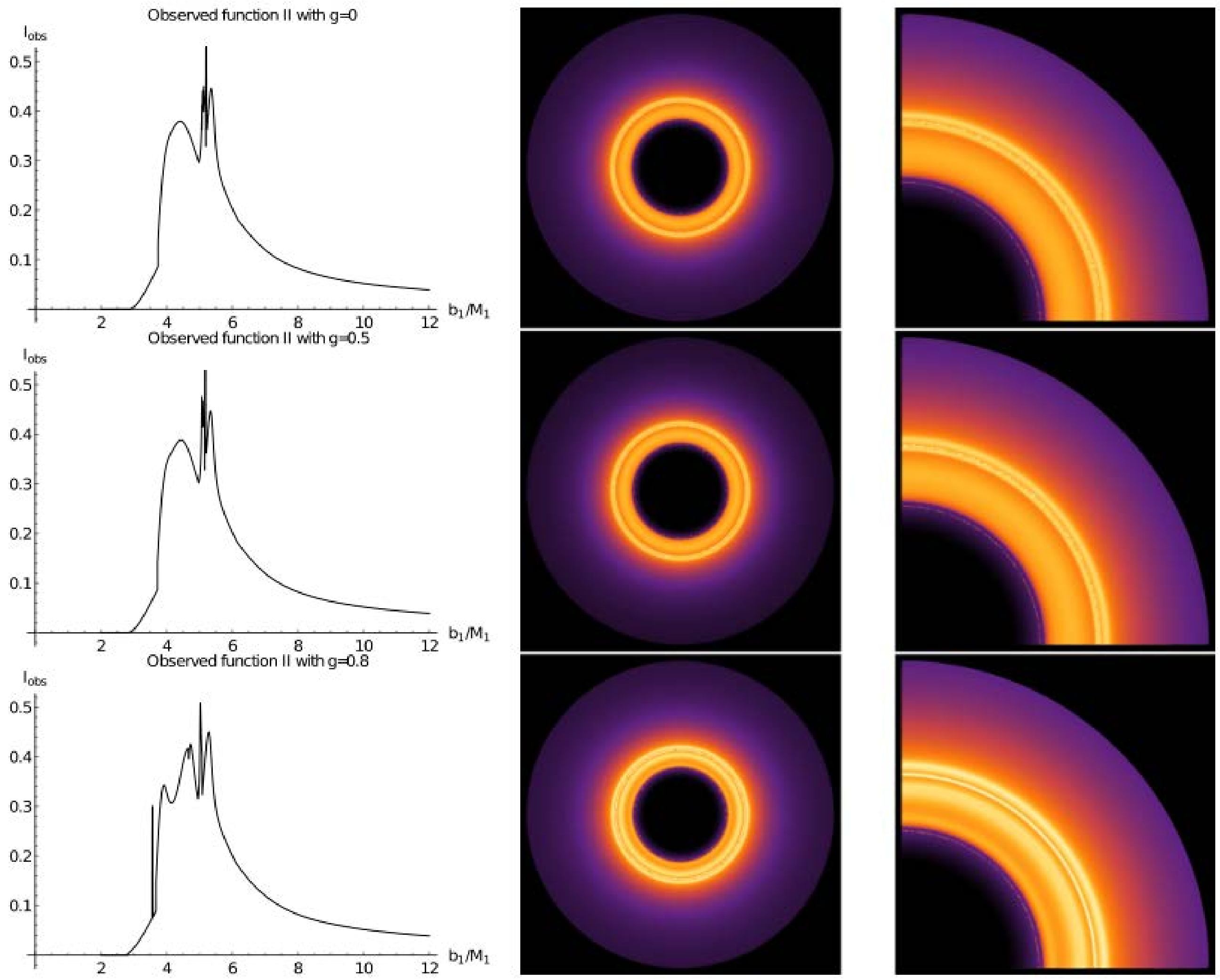

Fig 25: Optical appearance of TSW with a Hayward profile

Summary

- The accretion does not affect the radius of the photon sphere, which means that the black hole shadow is a geometric feature of spacetime.
- The observable characteristics of the BH surrounded by the thin disk accretion depend on both the BH spacetime structure and the position of the radiating accretion disk with respect to the BH.
- The optical appearance of a black hole surrounded by a thick accretion disk depends on the observation angle.
- In addition to spherically symmetric black holes, the optical appearance of rotating black holes surrounded by different accretions is also worth studying, and the results are closer to the EHT observation results.